151403

İSTANBUL TECHNICAL UNIVERSITY ★ INSTITUTE OF SCIENCE AND TECHNOLOGY

DETERMINATION OF TRANSONIC FLOW PROPERTIES OF ITU TRISONIC WIND TUNNEL

M. Sc. Thesis by
Ahmet SAYIN, Aeronautical Eng.

(708011005)

Date of submission : **26 April 2004**

Date of defence examination: **20 May 2004**

Supervisor (Chairman): **Asst. Prof. Dr. Okşan ÇETİNER-YILDIRIM**

Members of the Examining Committee **Asst. Prof. Dr. K. Bülent YÜCEİL**

Prof. Dr. İ. Bedii ÖZDEMİR

MAY 2004

151403

İSTANBUL TEKNİK ÜNİVERSİTESİ ★ FEN BİLİMLERİ ENSTİTÜSÜ

İTÜ TRİSONİK RÜZGAR TÜNELİNİN TRANSONİK AKIŞ ÖZELLİKLERİNİN BELİRLENMESİ

YÜKSEK LİSANS TEZİ

Havacılık Müh. Ahmet SAYIN

(708011005)

Tezin Enstitüye Verildiği Tarih : 26 Nisan 2004
Tezin Savunulduğu Tarih : 20 Mayıs 2004

Tez Danışmanı : **Yrd. Doç. Dr. Okşan ÇETİNER-YILDIRIM**

Diğer Jüri Üyeleri **Yrd. Doç. Dr. K. Bülent YÜCEİL**

Prof. Dr. İ. Bedii ÖZDEMİR

Mayıs 2004

FOREWORD

ITU 150mm×150mm Trisonic Wind Tunnel is an intermittent blowdown type wind tunnel and is capable of covering Mach number ranges of 0.4 - 2.2 and 2.4 - 4.0. In this study, at first the calibration of the tunnel transducers are redone. Then, some experiments are done to find total pressure distributions at transonic flows and static pressure measurements at the design Mach number of the tunnel in the test section. Finally, the repeatability of the results is checked.

I would like to express my sincere gratitude to my supervisor Asst. Prof. Dr. Oksan N. L. CETINER – YILDIRIM and my co-supervisor Asst. Prof. Dr. Kemal Bulent YUCEIL for their guidence and support. Their dedication to greatness and care has allowed this work to be completed.

I will forever be grateful to my family for their unconditional love and teaching me the value of learning.

I am thankful to staff of Trisonic Research Center, Asst. Prof. Dr. Hayri ACAR, Asst. Prof. Dr. Duygu ERDEM, Murat SARITAS, M. Ceylan TOPAL, Egemen TINAR, Onur Şişmangil, Idil FENERCIOGLU, Hakan GUNES, Ali Osman TABANLI, Ahmet SAVAS and Muslum CAKIR for their endless support and the times they had spared for me and for my work.

And finally, I will never forget the three years that have passed in Zeynep Birkan. We shared, we laughed, we learnt and we grew up. I hope we will always remember what we have shared, what we have laughed at, what we have learnt and who we have grown into.

April 2004 Ahmet Sayin

TABLE OF CONTENTS

LIST OF TABLES

LIST OF FIGURES

İTÜ TRİSONİK RÜZGAR TÜNELİNİN TRANSONİK AKIŞ ÖZELLİKLERİNİN BELİRLENMESİ

ÖZET

İTÜ 150mm×150mm Trisonik Rüzgar Tüneli, 0.4 - 2.2 ve 2.4 - 4.0 Mach sayısı aralıklarında istenilen hızda deney yapmaya olanak tanıyan bir tüneldir. Değişik deney şartlarını sağlaması açısından boğaz açıklıklarının değişebilir olması gerekmektedir. Bu özellik avantaj gibi görünmesine rağmen birçok kez akış kalitesini kötü yönde etkilemektedir.

Bu çalışmada, öncelikle tünelin mevcut basınç duyargaları kalibre edilmiştir. Daha sonra deney odasındaki toplam ve statik basınç dağılımı elde edilerek akım kalitesi bulunmaya çalışılmıştır. Toplam basınç ölçümleri 0.7 – 1.3 Mach sayıları arasında yapılırken, statik basınç ölçümleri sadece 2.2 Mach sayısında yapılmıştır. Son olarak statik basınç ölçümleri esas alınarak deney şart ve sonuçlarının tekrarlanabilirliği üzerinde durulmuştur.

DETERMINATION OF TRANSONIC FLOW PROPERTIES OF ITU TRISONIC WIND TUNNEL

SUMMARY

ITU Trisonic Wind Tunnel is capable of covering Mach number ranges of 0.4 - 2.2 and 2.4 - 4.0. Although continuous variation of throat areas seems to be advantageous in terms of experimental capabilities, it adversely affects the flow quality.

In this study, pressure measurements are performed to determine the flow quality within the test section of the 150x150 Trisonic Wind Tunnel using total or static pressure probes attached to a traversing system. At first the calibration of the tunnel transducers are redone. Then, some experiments are done to find total pressure distributions at transonic flows and static pressure measurements at the design Mach number of the tunnel in the test section. Finally, the repeatability of the results is checked.

1. INTRODUCTION

ITU 150mm×150mm Trisonic Wind Tunnel is an intermittent blowdown type wind tunnel built in the early 80's. Although the original producer of the tunnel, SESSIA, a French company, is no longer in business, limited support for certain part is available from another company. The tunnel has two interchangeable nozzle-test section blocks, which enable continuously covering two Mach number ranges of 0.4 - 2.2 and 2.4 - 4.0 by installing appropriate block. The tunnel is equipped with a 3-component sting type balance for measurement of drag, lift and pitching moment and a motorized arc mechanism to adjust the angle of attack of test models within 15°.

There are certain facts that affect the utilization of the tunnel for a wide range of applications [10]. They can be summarized as follows:

i. Although the continuous variation of the first and second throat areas seems to be advantageous in terms of experimental capabilities, such as having a range of operational Mach numbers, it has an adverse effect on the flow quality especially in transonic regime.

ii. The cross sectional size of the test section, which is 150 mm by 155 mm (W × H), limits the use of the tunnel to relatively small axisymmetric test models.

iii. The duration of the experiments is limited to less than a minute for high Mach number flows and a few minutes for subsonic compressible flows.

iv. As the tunnel's establishment dates back to early 80's and it is bought as a turn-key system, the repair and replacement processes can take a considerable amount of time compared to that spent for research, and also the implementation of new measurement techniques and tools becomes relatively difficult.

The following pieces of information on the wind tunnels are taken from reference [5] and given in quotes: "Wind tunnels are devices which provide an airstream flowing under controlled conditions so that items of interest to aeronautical engineers can be tested. High-speed tunnels are those usual operating speeds require the inclusion of compressible flow effects. This means that in the high-speed field we usually talk about 'Mach number'- the ratio of a given velocity to the speed of sound in the air about the body- as a more typical parameter than velocity. A lower limit of 'high speed' might be considered to be where the Mach number is approximately 0.5.

The power to drive a low-speed wind tunnel varies as the cube of the velocity in the wind tunnel. Although this rule does not hold into the high-speed regime, the implication of rapidly increasing power requirements with increasing test speed is correct. There are two types of high-speed wind tunnels, intermittent type and continuous type. Because of the power requirements, high-speed wind tunnels are often the intermittent type, in which energy is stored in the form of pressure or vacuum or both and is allowed to drive the tunnel only a few seconds out of each pumping hour.

There are mainly three types of intermittent tunnels, which are blowdown, indraft and pressure-vacuum tunnels. The intermittent blowdown and indraft tunnels are normally used for Mach numbers from 0.5 to about 5.0, and the intermittent pressure-vacuum tunnels are normally used for higher Mach numbers." Since the ITU 150mm×150mm Trisonic Wind Tunnel is an intermittent type wind tunnel, it will be useful to mention the advantages of this type wind tunnels.

"Advantages claimed for intermittent tunnels are:

1. They are simpler to design and less costly to build.
2. A single drive may easily run several tunnels of different capabilities.
3. Model testing is more convenient, since a lot of time need to be spent in pumping down the whole circuit and getting the drive motors up to spend.
4. Failure of a model will usually not result in tunnel damage.
5. Extra power is available to start the tunnel. Less power is needed according to continuous tunnels.

6. Loads on a model during the establishment of high-speed flow are less severe because of faster starts.

There is little choice in the type of the intermittent tunnel to be used at the higher Mach numbers. The compression ratio requirements are so high that a pressure-vacuum tunnel is dictated. It is not practical to operate with atmospheric inlet pressure (as with the indraft tunnel) or with atmospheric discharge pressure (as with the blowdown tunnel). However, there are many high-speed wind tunnels operating at Mach numbers for which both the indraft and blowdown tunnel are practical. Lists of the advantages of these two types of tunnels when compared with each other follow.

Some advantages of the indraft tunnel over the blowdown tunnel are:

1. Total air temperature at supply conditions is constant during a run.
2. Total air pressure at supply conditions is constant during a run although it may be lower than desired. There are no variations in total pressure such as those a pressure regulator may cause.
3. The airstream is free from contaminants such as compressor oil.
4. The headaches and dangers of pressure regulators are removed.
5. Loads on a model during the establishment of the high-speed flow are smaller.
6. Vacuum is safer to handle than pressure.
7. The noise level is lower.
8. Obtaining low air density in the tunnel is not difficult.
9. The indraft tunnel can operate at higher Mach numbers before heating is required to prevent the liquefaction of air during the expansion to high speeds.
10. For a given cost, indraft tunnels are larger.

Advantages of the blowdown tunnel over the indraft tunnel are:

1. It is possible to vary the Reynolds number widely at a particular Mach number. In some cases the value corresponding to full-scale flight may be reached.

2. Cost is from slightly lower than to less than one-fourth of that of an indraft tunnel of equal Reynolds number.
3. Short-time burning tests are usually possible. "

This study focuses especially on the results and observations made for the calibration of the original tunnel transducers, total and static pressure distribution in the test section, and summarizes problems encountered in measurements and the chronological study carried out to address them. Additionally, the repeatability of the results is checked.

2. LITERATURE REWIEV

Transonic flow, due to its being a transitional flow regime between the purely subsonic and supersonic flows, presents a wide range of complex flow features and problems such as shock waves and their interaction with bodies and boundary layers. Determination of transonic flow properties of ITU trisonic wind tunnel constitutes the subject of this study; therefore it is important to refer to some of the significant studies which define the theoretical concepts of transonic aerodynamics such as those by Ferrari and Tricomi [1], Ramm [2] and Moulden [3].

To give an insight on the experimental investigations at transonic speeds, Blackwell [4] presents a state-of-the art review of experimental testing at transonic speeds with particular emphasis on problems and ways used to minimize or solve them.

Also, determining the characteristics of a wind tunnel is of vital importance. Pope [5] has stated that the calibration of a supersonic wind tunnel includes determining the Mach number, flow angularity and turbulence level in the wind tunnel.

Gulacti [6] carried out in the ITU 150 x 150 Trisonic Wind Tunnel flow visualization, pressure and force measurements at two different Mach number – M=2.67 and M=3.13.

Elbay [7] carried out a doctoral study on understanding and improving the computer program and the calibration of all the components of the ITU 150 x 150 Trisonic Wind Tunnel. During the study, the computer program for the operation of the tunnel was improved and simple experiments were made at a freestream Mach number of 3.0 to determine the flow quality of the tunnel. For this purpose, total and static pressures were measured at the mid section of the tunnel. After this survey, it was observed that the total and static pressure along the test section of the tunnel remains constant.

In the previous studies on the tunnel, the test section providing a Mach number range of 2.4 - 4.0 had been used. It has the simplicity of having one parameter for velocity-throat area calibration. Due to a demand of the tunnel use at transonic speeds for a missile aerodynamics project, the test section of the tunnel was replaced with the other test section providing a Mach number range of 0.4 – 2.2. The wind tunnel has originally a 3-stage compressor which had several breakdowns and thus limited the research efforts in terms of time and funding. Most of the studies done in this facility have been supported by the State Planning Organization and have been in the context of fundamental research [8, 9].

Sayin et al [10] conducted a preliminary study which focused especially on the results and observations made for the total and static pressure distribution in the test section. They identified the problems encountered in measurements and the provided the results obtained from the chronological study carried out to address them.

3. EXPERIMENTAL SETUP

All experiments were conducted at the 150 × 150 Trisonic Wind Tunnel, located at the Istanbul Technical University Trisonic Research Center (TAM). This chapter presents basic description of the wind tunnel, the models and the instrumentation, which were used in the experiments.

3.1 Wind Tunnel and Components

The 150 × 150 Trisonic Wind Tunnel is an intermittent blowdown type wind tunnel with test section area of 150mm × 150mm × 400mm. The schematic layout of the wind tunnel can be seen in Figure 3.1.

Air is stored in two identical pressure tanks with internal volumes of 27 m^3 each. Tanks are filled upto 40 bars using In the first phase of the experiments, the original a three-stage tunnel compressor, is used. Later, a new screw-type compressor is installed and these two compressors have worked parallel. Although air is compressed up to 40 bars by the original compressor, in the first phase of the experiments tanks were filled up to 20 bars by using only the first two stages of the compressor. The new compressor is composed of two stages and can compress air up to 40 bars. One pneumatically controlled and two manually operated isolating valves separate tanks from the wind tunnel [9].

A pneumatically controlled regulation valve, which is located between the tanks and the stagnation chamber, keeps the stagnation pressure within a range suitable for the run conditions. In the experiments, the maximum opening and closing durations of the regulation valve have been deemed as important factors in regulating the stagnation chamber pressure and both should be adjusted to a value between 6s and 7s.

The security membrane on top of the stagnation chamber is made of nickel. It is 30.48 cm in diameter and it is designed to rapture at internal pressure above 5 bars at 20^0C to avoid dangerously high pressures in the stagnation chamber.

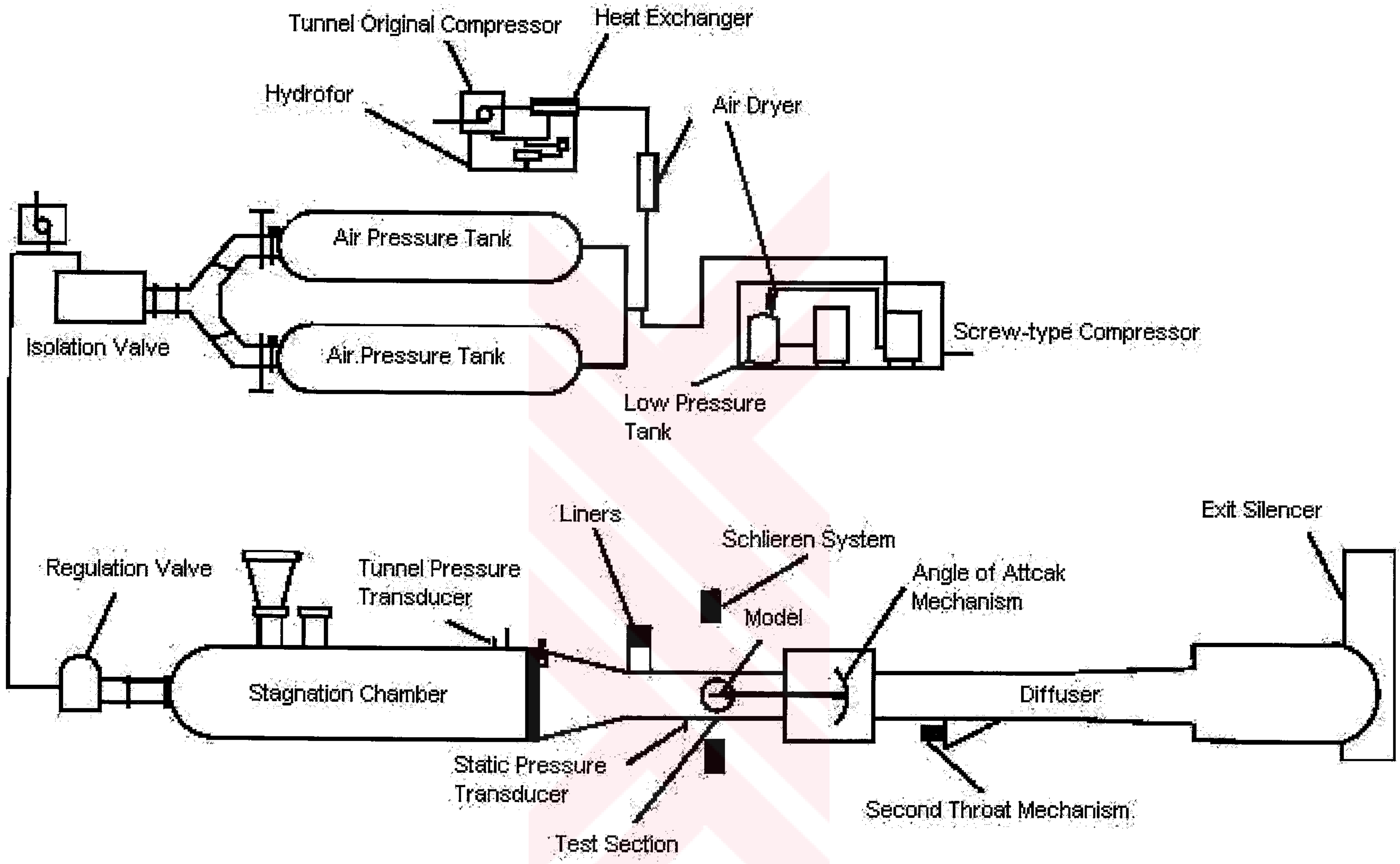

Figure 3.1 : The layout of 150 x 150 Trisonic Wind Tunnel

The nozzle test section assembly used in the experiments provides a Mach number range of 0.4 - 2.2. The test section is 1.960 m long and it includes an adjustable first throat and a test chamber with a boundary layer suction device for transonic flow regime. The first throat is bounded by the two side walls 150 mm apart and by two upper and lower walls converging down to the test section and thus varying the Mach number. The liners are used to change the throat area. A motorized mechanism is used to control the displacement of liners. Facing the model location, the side walls of the test section are equipped with 210 mm diameter round portholes fitted with Schlieren-quality glass window. The portholes are mounted on hinges with a sealing and locking system.

Operation of the wind tunnel, including controlling of the valves and throat mechanism, is performed via a computer program running on a PC. The computer performs the data acquisition required for the basic operation of the wind tunnel as well as acquiring balance data during the run.

The 3-component sting-type balance for force measurements is mounted on the angle of attack mechanism downstream of the test section. It has an automatic suction system for transonic operations and a device for changing the model incidence having an angle of attack range of -5^0 - $+10^0$.

The optical system used for flow visualization is the Schlieren system. This system gives an image representative of the variation of density throughout the complete flow field of the test section. Light from a point source (500 W) is collected into a parallel beam by two concave and convex mirrors and passes through the wind tunnel test section. The parallel beam is then focused on a knife edge and used to develop an image on a screen.

3.2 Flow Conditions

The duration of the experiments is limited to less than a minute for high Mach number flows and a few minutes for subsonic compressible flows.

The adjustment of the Mach number is done through the first and second throat. In the experiments, in which the Mach numbers are between 0.4 and 0.9, only the second throat is active. In the transonic region, between 0.9 and 1.1, the first and second throats are used together to adjust the Mach number in the test section. In the supersonic region, between 1.1 and 2.2, only the first throat is used.

Tunnel compression ratio, which is the ratio of the tunnel stagnation pressure to the atmospheric pressure, is one of the main parameters of the wind tunnel testing. Figure 3.2 shows the variation of the tunnel compression ratio with Mach number [5].

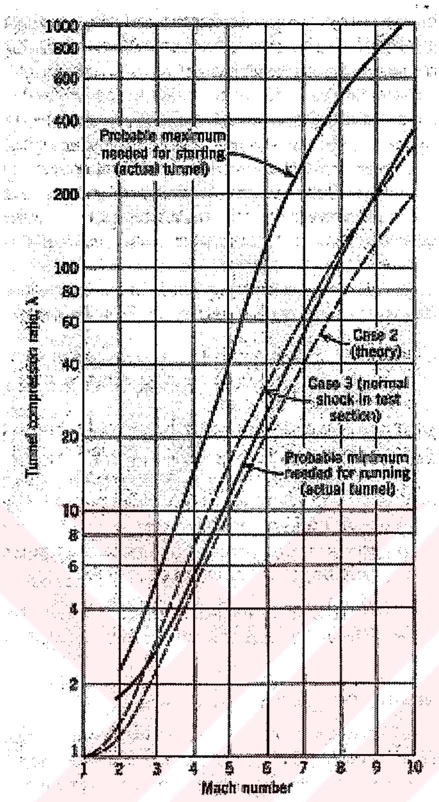

Figure 3.2: The variation of tunnel compression ratio with Mach number from [5].

3.3 Setup and Equipment for Pressure Distribution Measurements

Figure 3.3 shows the schematic of the test section with a separate block called "probe traversing insert" attached to the downstream of the test section to perform pressure surveys with using either a total pressure (pitot) probe or a static pressure probe. Figure 3.3 also shows the locations of the wall static pressure tap, static probe measurement area and the total probe measurement area. Total or static probe is mounted to the probe support which is located in the middle of the test section and can be moved up and down in vertical direction by using the infinite screw mechanism of the traverse system.

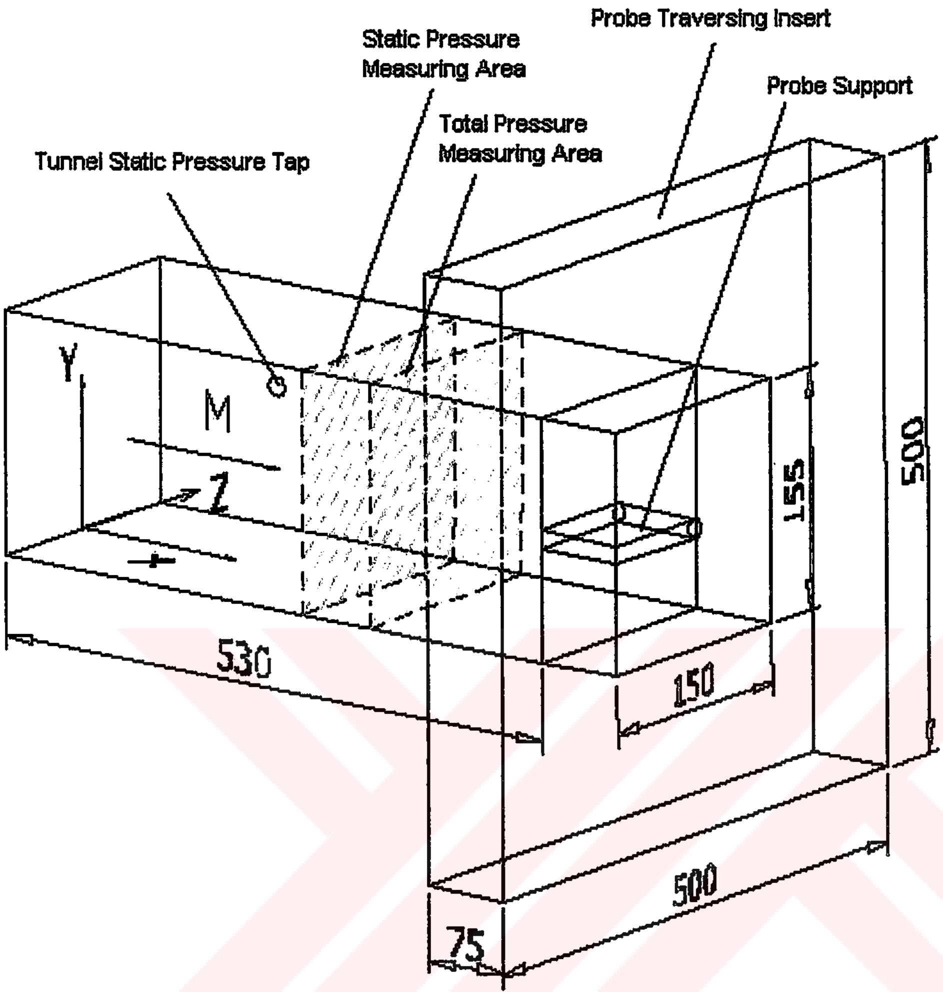

Figure 3.3 : Schematic of the test section and the probe traversing insert

A photograph of the probe traversing insert is shown in Figure 3.4.a. Attached to the screw mechanism a linear potentiometer, which is shown on the right side of the block in the figure, provides the distance information in terms of a linearly varying voltage. Photographs of the total pressure probe and the static pressure probe are shown in Figure 3.4.b and 3.4.c, respectively. The lengths of the probes are 154 mm and 300 mm, respectively. The maximum outer diameter of the probes is the same and 9.5 mm at their end. In the experiments, only the probes are used and the blockage ratio is calculated to be 0.3%. As can be seen from the Figure 3.3, measurements locations of total pressure probe, static pressure probe and the wall static pressure are different. In order to bring the measurement point of the static probe to the same location as the wall static pressure tap an extension adaptor (Figure 3.4.d) is made and used with the probe. The length of the probe extension adaptor is 184 mm and inner and maximum outer diameters are 8 mm and 18 mm, respectively. The blockage ratio is %1.09 when the extension adaptor is used in the experiments.

In order to make pressure measurements at the center of the test section without using the probe traversing insert another suitable adaptor (Figure 3.4.e) is manufactured. This adaptor is used to mount the probes to the model support so that single point measurements can be made. The length of the adaptor is 220 mm and inner and maximum outer diameter is 8 mm and 30 mm, respectively. The blockage ratio is %3.03 when this adaptor used in the experiments.

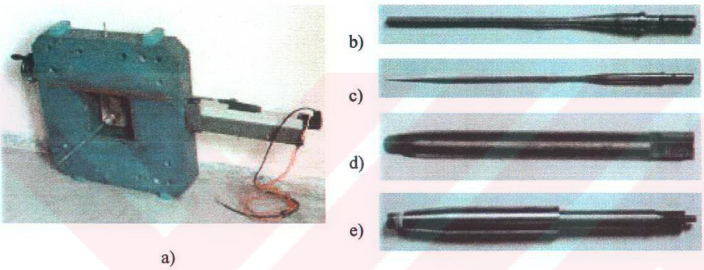

Figure 3.4 : Traverse system, probes and extension adaptors
a) Probe traversing insert, b) total pressure probe, c) static pressure probe,
d) probe extension adaptor, e) support extension adaptor

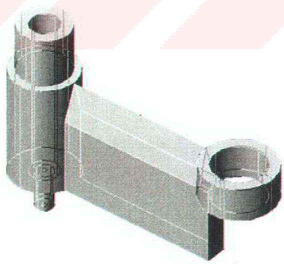

Figure 3.5 : Horizontal probe support adaptors

In order to make pressure measurement at the different horizontal positions of the test section another adaptor (Figure 3.5) is used. By mounting this adaptor to the probe support with different angles, total and static pressure distributions can be obtained over an area of 130mmx130mm in the test section.

The tunnel stagnation chamber pressure, wall static pressure and tank pressure are measured using respectively Gould Statham model PL 822-200 (0-13.79 bar - absolute), PM 822±50 (±3.44 bar - absolute) and PL 822-750 (0-51.71 bar - absolute) pressure transducers, which are thin film strain gage pressure transducers, respectively. Lines from total pressure and static pressure probes are connected to PCB model piezotronics type 1502C (0-13 bar - gage) and 1502C (0-4 bar - absolute) pressure transducers.

The position of the probe in the test section is measured using LPH model linear position transducer produced by Opkon Ltd. Its resistance is 10 kOhm. The resistance tolerance and linearity of the transducer are ± 20 % and ± 1 %, respectively.

3.4 Tunnel Control and Data Acquisition

The 150 × 150 Trisonic Wind Tunnel has a 16-channel data acquisition system for the basic operation and measurements during the tunnel run. Data acquisition system also provides analog and digital outputs for controlling the valves and switches of the wind tunnel system. Tank pressure, stagnation pressure, static pressure, angle of attack and balance (strain gage) outputs are among the quantities that are measured during the run. These signals are passed through amplifiers and signal conditioners before they are transmitted to the data acquisition board on the tunnel control computer.

3.4.1. Computer Programs

The details of the computer programs that are used to operate the 150 × 150 Trisonic Wind Tunnel will not be given here, however, some of the subroutines will be mentioned briefly. All of the control subroutines are written in FORTRAN language. During the course of an experiment, the main program TUNNEL calls the subroutine SPTRBIS in which the A/D converter starts reading the data from the 16 input channels. The voltage data are then converted to physical quantities by CEFFOR which uses the calibration coefficients that were stored in a data file called DATAPOL. The calibration coefficients were supplied subsequent to calibration process which was carried out prior to the experiments.

3.4.2 Data Acquisition System

Since the tunnel control program gives only the mean values for the measured quantities at certain instances during the run, it was inadequate for the current study in which the time history of the various pressures acting on the body was desired. Therefore, another data acquisition board on a separate computer is used to acquire the time history of the pressure data. A National Instruments model NI-6110 data acquisition board is controlled with in-house written LabView VI's.

The NI-6110 data acquisition board has 4 simultaneously sampled analog inputs. Its maximum sampling rate is 5 million samples per second per channel and maximum output range is 4 million samples per second for a single channel and 2.5 million samples per second on a dual-channel. The input range is between ±0.2 V and ±42 V and the output range is ±10 V. Its input and output resolutions are 12 bits and 16 bits respectively. It has 8 channels for digital input and output.

4. RESULTS

During the course of this study, two main types of pressure measurements were performed; Total and static pressure measurements. In this section, the results from these experiments will be discussed.

4.1. Pressure Transducer Calibrations

Before the experiments, the calibrations for the four strain gage type pressure transducers, that are used to measure the stagnation chamber pressure, static pressure at the side wall of the test section, fairing pressure at the aft of the balance support, and the pressure at the tunnel storage tanks, were redone by using two new certified pressure transducers and the calibration curves are shown in figure 4.1. It is found out that the new coefficients were not much different from the previous ones. The new calibration coefficients are entered in the tunnel control program.

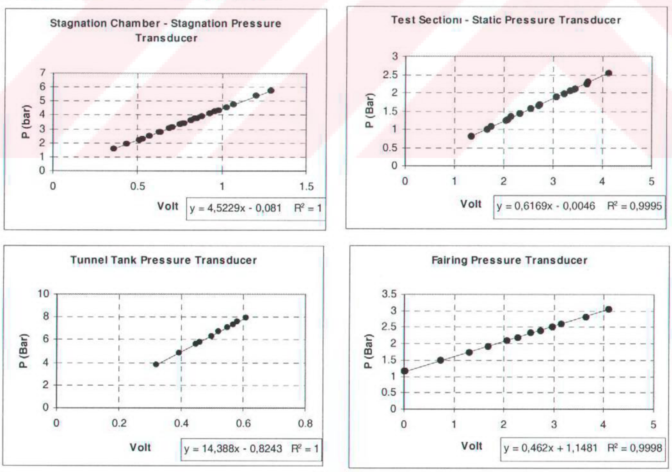

Figure 4.1 : The calibration curves of tunnel's transducers and new calibration coefficients

As mentioned earlier, pressure signals are measured by the new transducers (PCB model) besides the tunnel's original transducers in the experiments. The calibration curves and coefficients of the PCB transducers, used in the experiments, are shown in Figure 4.2.

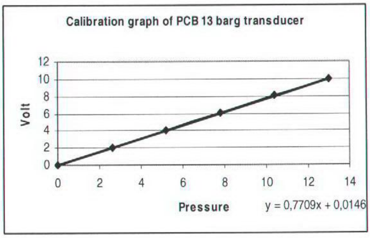

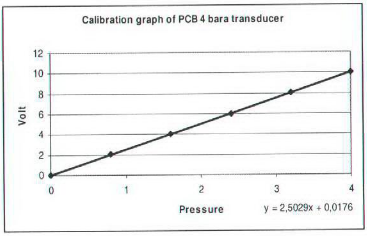

Figure 4.2 : The calibration curves of PCB transducers and calibration coefficients.

Besides the tunnel transducers, the distance transducer was also calibrated in each experiment when the probe traversing insert was used and the calibration curve is shown in Figure 4.3.

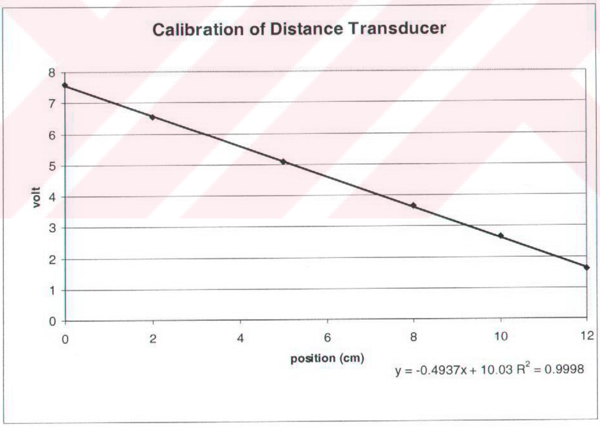

Figure 4.3 : The calibration curve of the distance transducer and the calibration coefficient

4.2 Total Pressure Distributions

In parallel with the stagnation chamber pressure measurements, total pressure probe is moved in vertical direction to obtain the total pressure distribution in the test section. Continuous time series data of total pressure, probe location, stagnation and wall static pressures have been collected using a separate data acquisition system. Mach number setting is varied between 0.7 and 1.3 for these experiments. The minimum distance between the probe and the tunnel wall was 10 mm due to relatively large diameter of the probe support.

The maximum duration of the experiments in obtaining the total pressure distributions was 70 seconds. In about 45 seconds of this duration, the steady conditions could be obtained. Tank pressure decreases about 14 bars during a typical run in these experiments. When the tank pressure drops below 5 bars, the tunnel is shut down and the data acquisition is terminated by the user due to inadequate operation of the regulation valve.

Although the first and the second throat can be used together in the adjustments of Mach number in transonic region, only the first throat is used in the present study and, the second throat is fully opened.

During the tunnel operation, once the flow conditions are steady and constant, the tunnel operating system gives a signal and waits for the user to acquire data. The Mach numbers of each experiment have been determined through the tunnel data acquisition system and checked with a separate measurement made with the total pressure probe outside the boundary layer.

Data acquisition rate for the total pressure probe surveys was 1000 samples/sec and is found to be excessive for such mean measurements and the data presented herein were filtered using a 5 Hz digital low-pass filter. The noise level at data acquisition channels has been determined by taking pressure data with no flow. In this case, the standard deviations are calculated to be 0.0013 bars for static wall pressure and 0.0053 bars for stagnation pressure; values for remaining channels were negligibly small. For the experiments, the standard deviations for wall static and tunnel stagnation pressures were in the range of 0.0009 – 0.006 bars and 0.003 – 0.02 bars, respectively.

Total pressure values obtained from the probe have been directly used to calculate the Mach numbers assuming isentropic compression in front of the probe since the flow speeds are close to sonic conditions for all the experiments. The maximum error in this assumption is found not to exceed 1.2% at the highest Mach number of 1.3.

The direction of the movement of the total probe is not always the same in the experiments. However, it can be deduced from the probe location line obtained from the linear transducer and drawn with other tunnel pressure characteristics.

Figure 4.4.a shows the variation with tunnel run time of total pressures obtained from the tunnel stagnation chamber and the pitot probe along with the wall static pressure and the vertical location of the pitot probe at a nominal run Mach number of 0.7. As can be seen from the figure, the agreement between the two total pressures is quite good considering the values are measured using different locations and different transducers. In Figure 4.4.b vertical distributions of pitot total pressure and tunnel stagnation pressure are plotted. In Figure 4.4.c vertical distribution of Mach number calculated using the pitot total pressure and the Mach number calculated using the tunnel stagnation pressure are plotted. Tunnel wall static pressure is used in both calculations. As mentioned above, it is not possible to go any closer to the upper and lower walls due to the size and limitations of the probe used. At this tunnel speed setting, the distributions of Mach numbers are very uniform and in good agreement with each other. At about 3 cm away from both walls probe pressure starts fluctuating due to probe entering the turbulent boundary layer developing over the tunnel walls.

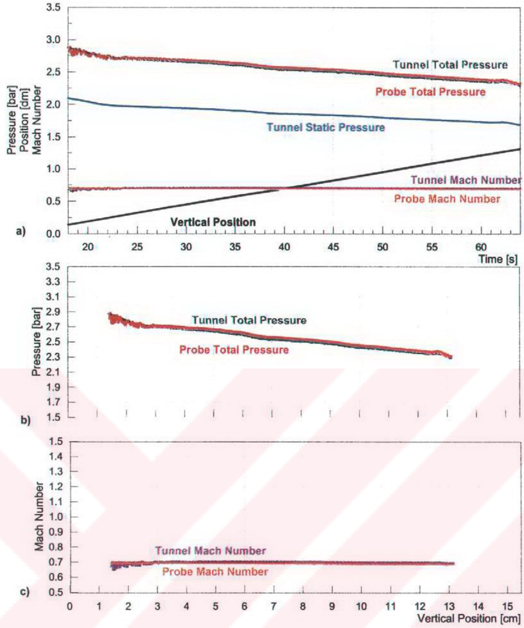

Figure 4.4: Total pressure probe measurements for M = 0.7.
a) Time histories, b) Vertical variation of Total Pressure,
c) Vertical variation of Mach number

In Figure 4.5, variations of same quantities are shown for a nominal Mach number of 0.9. Except for the regions close to the walls the agreement between the probe measurements and the tunnel stagnation chamber measurements is very good. The effect of boundary layer in terms of lower and fluctuating values of Mach number can be seen at about 2.5-3 cm from the walls. In the inviscid flow region spatial distribution of Mach number (Figure 4.5.c) is quite uniform although a slight drop in the value can be visualized.

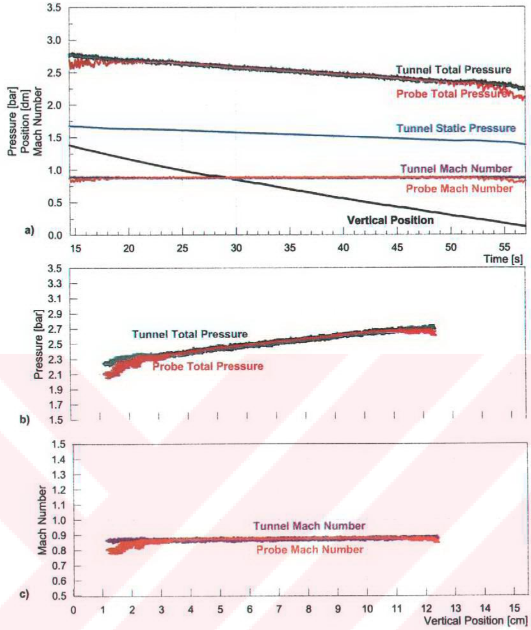

Figure 4.5: Total pressure probe measurements for M = 0.9.
a) Time histories, b) Vertical variation of Total Pressure,
c) Vertical variation of Mach number

In Figure 4.6, variations of same quantities are shown for a nominal Mach number of 0.95. Similar to the former experiment, except for the regions close to the walls the agreement between the probe measurements and the tunnel stagnation chamber measurements is very good. The effect of boundary layer in terms of lower and fluctuating values of Mach number can be seen at about 2.5 cm from the walls.

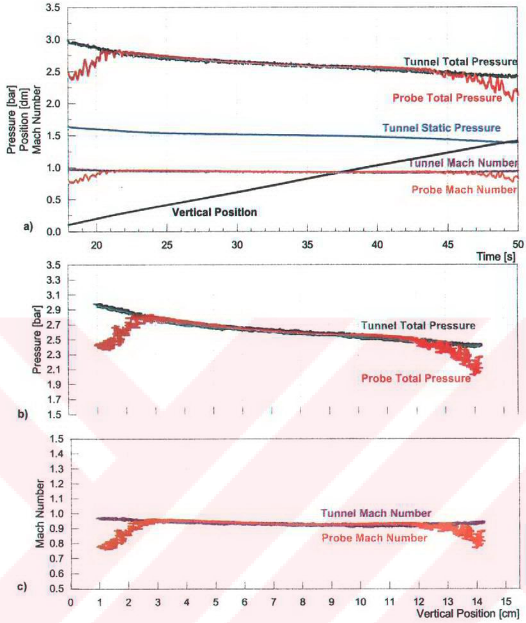

Figure 4.6: Total pressure probe measurements for M = 0.95.
a) Time histories, b) Vertical variation of Total Pressure,
c) Vertical variation of Mach number

In Figure 4.7, variations of same quantities are shown for a nominal Mach number of 1.0. In this experiment, initial position of the probe is 3.75 cm above the bottom of the test section and so the boundary layer effect is only seen on the top of the test section. Although obtaining uniform flow is very difficult in sonic flow, result of the experiment is satisfactory. Similar to previous experiments, the boundary layer thickness and the agreement between the total pressure and Mach number distribution except the boundary layer region is stable.

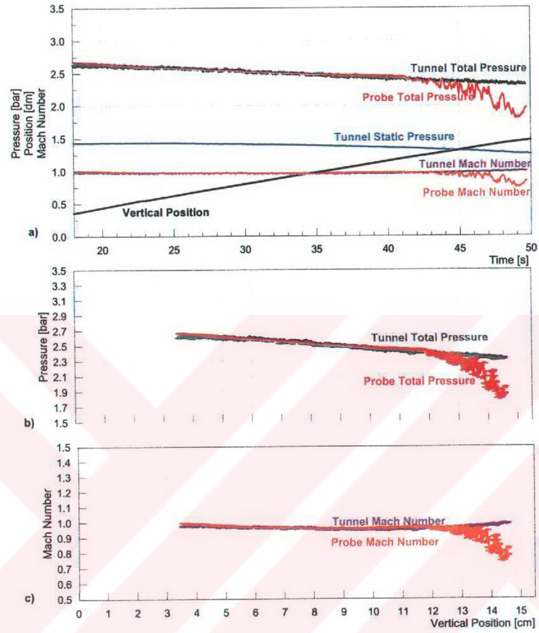

Figure 4.7: Total pressure probe measurements for M = 1.0.
a) Time histories, b) Vertical variation of Total Pressure,
c) Vertical variation of Mach number

In these three figures, variations of same quantities are shown for a nominal Mach number of 1.1. The Mach number values of the experiments in the Figures 4.9 and 4.10 are very different than 1.1 since in these experiments static pressure distribution is affected by the probe approaching to the tunnel wall. Although not seen in other Mach number cases, in this case bringing the probe close to the wall seems to affect the wall static pressure measured through the wall static pressure tap which is located considerably upstream (184 mm) of the tip of the total pressure probe. Except the positions, in which there are no shock wave effects, total pressure values from probe and stagnation chamber show good agreement. However, there is still difference between these values in the boundary layer region.

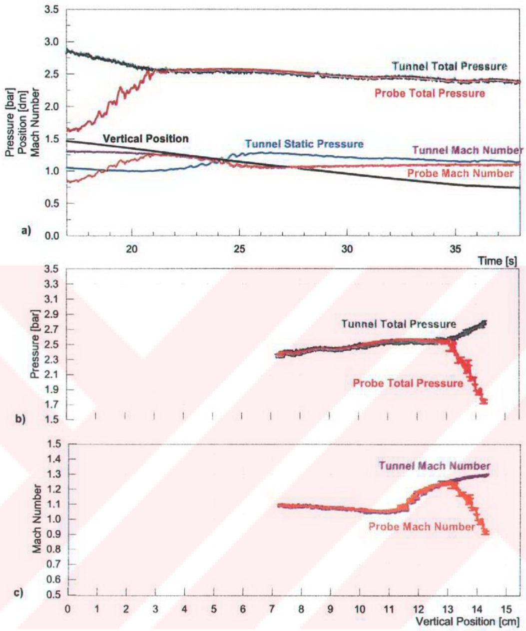

Figure 4.8: Total pressure probe measurements for M = 1.1.
a) Time histories, b) Vertical variation of Total Pressure,
c) Vertical variation of Mach number

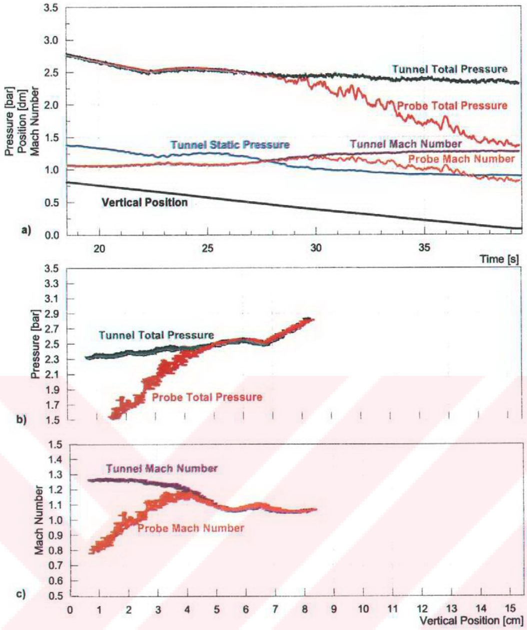

Figure 4.9: Total pressure probe measurements for M = 1.1.
a) Time histories, b) Vertical variation of Total Pressure,
c) Vertical variation of Mach Number

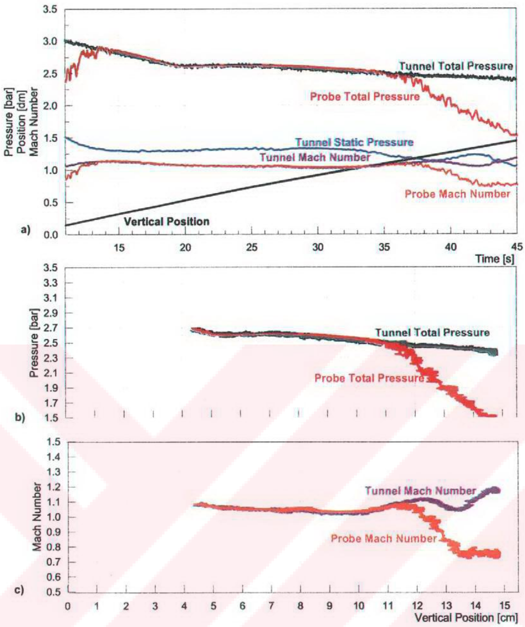

Figure 4.10: Total pressure probe measurements for M = 1.1.
a) Time histories, b) Vertical variation of Total Pressure,
c) Vertical variation of Mach number

Finally, Figure 4.11 shows the variation of the tunnel parameters for the nominal Mach number of 1.3. In contrast with the Mach 1.1 case, there is no indication of affecting the wall static pressure with the probe-wall proximity although the probe is brought 1-1.5 cm near the wall. Again, the agreement between the total pressures is quite good and the Mach number distribution (Figure 4.11.c) in vertical direction in the middle of the test section is very uniform. Since the probe enters the boundary layer at about 3 cm from the walls Mach number begins to decrease and fluctuate as seen in Figure 4.11.c.

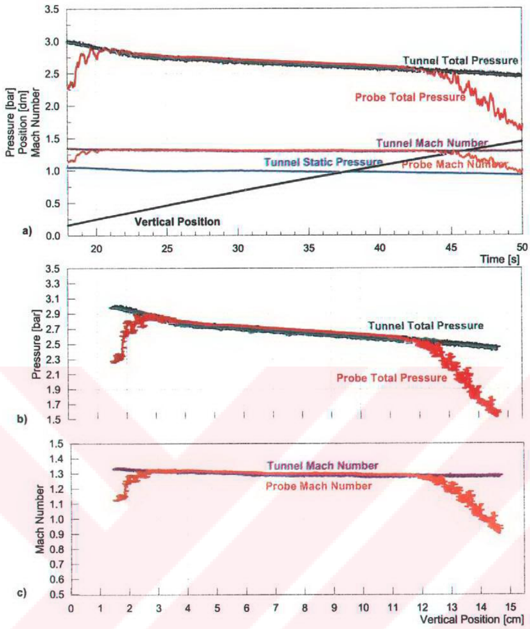

Figure 4.11: Total pressure probe measurements for M = 1.3.
a) Time histories, b) Vertical variation of Total Pressure,
c) Vertical variation of Mach number

4.3 Static Pressure Measurements

For the assessment of the static pressure distribution inside the test section, preliminary measurements were made by moving the static probe using the traverse system. However, these experiments showed a significant discrepancy between wall static and the probe static pressures for the period when the probe is stationary during the start and shut down of the tunnel. Therefore, for the rest of the experiments the probe was held stationary during measurements at the center of the test section.

The duration of the experiments in the total pressure distributions was about 22 seconds. The tunnel was run about 3-4 seconds after reaching the steady conditions in these experiments. The tank pressure is reduced about 5 bars in these experiments. When the tank pressure was less than 10 bars, data were not acquired. The flow rate in these experiments was about 4.16 kg/s.

Sampling rate for the static probe measurements is 100 Hz. However, due to high frequency noise present in the signals from tunnel stagnation and static pressure transducers time histories are presented by taking a running average using 21 data points, which has removed the noise without changing the character of the mean variations.

In order to obtain the same Mach number in the test section for all the experiments, the first throat is set to close down to its minimum area at each run. The Mach number obtained is expected to be the maximum design Mach number of this test section which is 2.2. However, early studies performed during the establishment of the tunnel suggest that the maximum value that can be obtained with this setting is slightly lower than 2.2. Although this case is the most reliable one in terms of the control of the throat area, the area value is checked and confirmed to be the minimum after each experiment. The compression ratio (P_m/P) is determined as 3.0 in the tunnel run directions.

4.3.1. Early studies on static pressure measurements

The chronological study to address the problems with static probe measurements can be presented in four cases with different configurations:

4.3.1.1 Probe traversing insert present, different measurement locations along the tunnel axis

This case constitutes the original setup for the determination of the flow quality in the test section, in which the probe is mounted to the probe traversing insert. As shown in Fig. 4.12, the wall static pressure tap and the static pressure holes on the probe are not at the same position, the former being 184 mm upstream.

As an example of two similar experiments done on the same day with the same conditions, Figures 4.13.a and 4.13b show the time histories of stagnation pressure and two static pressures, one which is obtained from the tunnel side wall and the other which is measured by the static probe. Also shown in the figures are the calculated Mach numbers using these two pressure values and the stagnation pressure. The duration of steady flow conditions which are suitable to make measurements at a constant Mach number is shown in between two dashed lines and the average Mach numbers in this duration are indicated on the figure. In these two runs there is a significant discrepancy between the two measured static pressures and thus the two Mach numbers calculated.

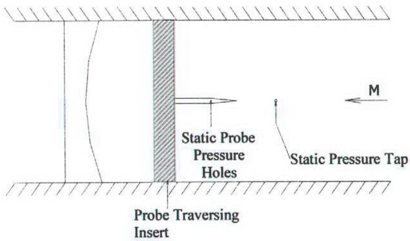

Figure 4.12: The schematic of the test section when the probe traversing insert is present and the wall static pressure tap and the static pressure holes are at different locations

In Figure 4.13.a Mach number obtained from the probe is almost constant at the value of 2.07 whereas that obtained from tunnel static pressure indicates a decrease from about 1.8 to 1.7. Figure 4.13.b shows a similar behavior. In both cases the values obtained from the probe are closer to the maximum design Mach number of the test section.

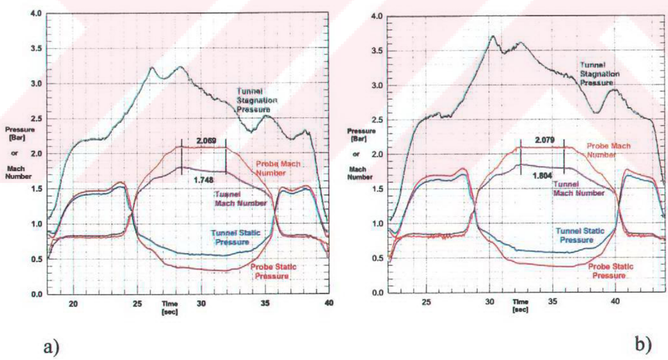

Figure 4.13: Static pressure probe measurements with insert present and different streamwise location of measurement points.
a) & b) Two time histories with the same run conditions

The reason for the difference between the two values is, although not proved, thought to be a leakage caused by the probe traversing insert. If there is such a leakage, then the higher pressure of the ambient may find its way to the pressure tap on the side wall through the subsonic portion of the wall boundary layer which in turn registers a higher value as shown in the figure.

4.3.1.2. Probe traversing insert present, same measurement locations along the tunnel axis

In this case, as shown in Figure 4.14, an extension to the probe support is manufactured in order to bring the probe static holes to the same location as the wall static pressure tap so that they would be at the same streamwise location and hence measure the same static pressure.

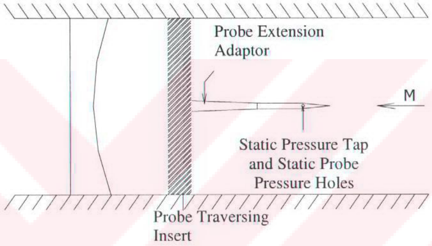

Figure 4.14: The schematic of the test section when the probe traversing insert is present and the wall static pressure tap and the static pressure holes are at the same positions

Figures 4.15.a and 4.15.b show results of two similar experiments performed the same day with the same conditions for this configuration. In contrast to the results shown in Figure 4.13, this case shows a good agreement in Mach numbers obtained from two static pressure sources although the probe traversing insert is present. There is still a slight difference with the same trend seen in the previous case but the discrepancy is now very small. Since these experiments were made at a different date from those of the previous case it is possible that the suspected leakage by the insert is minimized in this new configuration. This is also evident from the fact that the Mach number from the wall static pressure remains nearly constant as does the probe Mach number as can be seen from the figures. Another observation with this setup is that the Mach number, 2.135, obtained from the probe is much closer to the design Mach number of 2.2. This could be due to probe being located more upstream where the wall boundary layer thickness is smaller thus giving a larger area for the flow hence a higher Mach number.

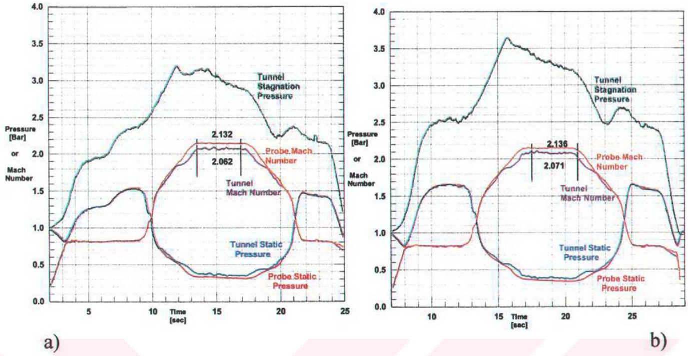

Figure 4.15: Static pressure probe measurements with insert present and the same streamwise location of measurement points.
a) & b) Two time histories with the same run conditions

4.3.1.3. Probe traversing insert absent, different measurement locations along the tunnel axis

In this case the probe traversing insert is removed from the test section to avoid the possibility of causing air leakage. The static pressure probe is mounted in the test section using the tunnel model support and it is shown in Figure 4.16.

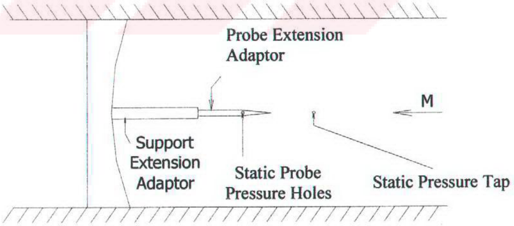

Figure 4.16: The schematic of the test section when the probe traversing insert is absent and the wall static pressure tap and the static pressure holes are at different locations

For this, an adaptor is manufactured to use with the model support and the pressure probe is mounted such that its static pressure holes are at the same location in the tunnel axis as would be if mounted with the traverse system.

Figure 4.17 shows the time histories of pressures and resulting Mach numbers with this configuration. As can be seen from the figure there is a good agreement between the two static pressures and hence the Mach numbers calculated. During the steady flow conditions the difference between the two Mach numbers in the test section is 0.08 which can be caused by some small leakage still present somewhere around the wall static tap.

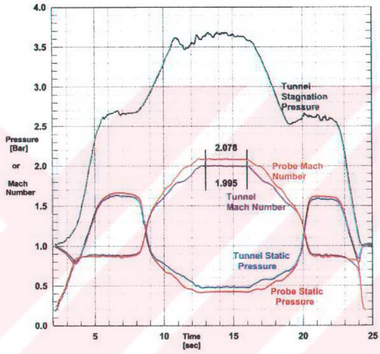

Figure 4.17: Static pressure probe measurements without the insert and different streamwise location of measurement points.

4.3.1.4 Probe traversing insert absent, same measurement locations along the tunnel axis

In this last configuration, as shown in Figure 4.18, the probe is mounted on the model support with another adaptor to bring the location of its holes forward to match with that of the wall static pressure tap.

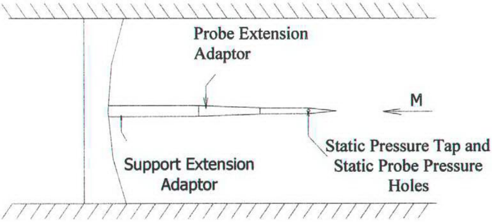

Figure 4.18: The schematic of the test section when the probe traversing insert is absent and the wall static pressure tap and the static pressure holes are at the same locations

The value of the Mach number calculated using the wall static pressure measurement is almost identical to that obtained in the previous case as can be seen in Figure 4.19. However, the value calculated by using the probe static pressure is increased by an amount of 0.07 due to probe being located more upstream with respect to the previous case as explained in the second configuration.

Figure 4.19 also shows that the Mach number stays relatively constant during the measurement-ready period in the test section, which indicates the quality of the flow conditions.

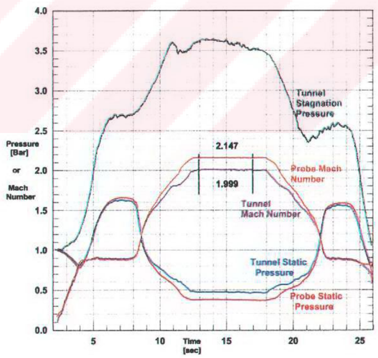

Figure 4.19: Static pressure probe measurements without the insert and the same streamwise location of measurement points.

Although the time histories of Mach numbers for all of the above cases show almost constant values, more experiments need to be performed to confirm this behavior. Due to the technical problems associated with the original tunnel compressor it was not possible to perform high number of runs for some time. After the installation of a new screw-type compressor for the tunnel, we could find possibility to continue the studies. In the mean time, we tried to investigate the reason of the leakage and changed some small parts of the tunnel, e.g. bolt of the static pressure tap.

4.3.2. Continued studies on static pressure measurements

After the installation of the compressor and changing some parts of the tunnel, the static pressure measurements were repeated according to these 4 different configurations and 2 different tunnel compression ratios. This time, totally, 23 experiments were done in these four configurations and two tunnel compression ratios. Although $P_m/P = 2.3$ is enough for running the tunnel, $P_m/P = 3$, which is the suggested compression ratio in the stagnation chamber for $M = 2.2$, is also used in the experiments to find the effect of the difference between these two ratios. Similar to the previous studies, sampling rate for the static probe measurements is 100 Hz. and time histories are presented by taking a running average using 21 data points. Also, the first throat is set to close down to its minimum area at each run to obtain the maximum design Mach number of the test section which is 2.2.

4.3.2.1. Probe traversing insert present, different measurement locations along the tunnel axis at $P_m/P = 2.3$

Figures 4.20.a and 4.20.b show the time histories of stagnation pressure and two static pressures (from wall and probe) of two experiments, which are done on the same day. Also, the variation of Mach numbers are calculated and plotted using these two pressure values and the stagnation pressure. In these two runs there is a little discrepancy between the two measured static pressures and thus the two Mach numbers calculated. In figure 4.20.a Mach number obtained from the probe is constant at the value of 2.093 whereas that obtained from tunnel static pressure is about 2.067. Figure 4.20.b shows a similar behavior. In both cases the values obtained from the probe are closer to the maximum design Mach number of the test section.

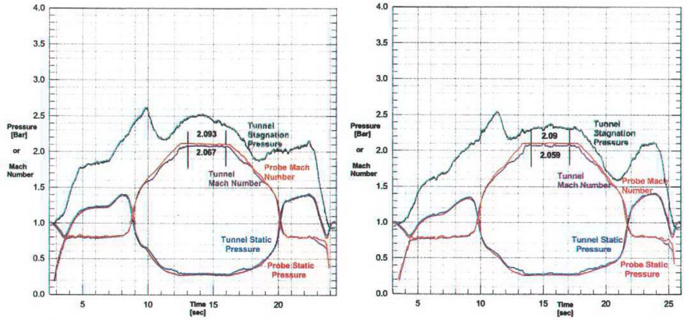

a) b)

Figure 4.20: Static pressure probe measurements with the insert and different streamwise location of measurement points at $P_m/P = 2.3$.

4.3.2.2. Probe traversing insert present, different measurement locations along the tunnel axis at $P_m/P = 3$:

The experiments, shown in Figures 4.21.a and 4.21.b, are done on the same day and on the same test conditions. In these two runs there is a perfect consistency between the two measured static pressures and thus the two Mach numbers calculated.

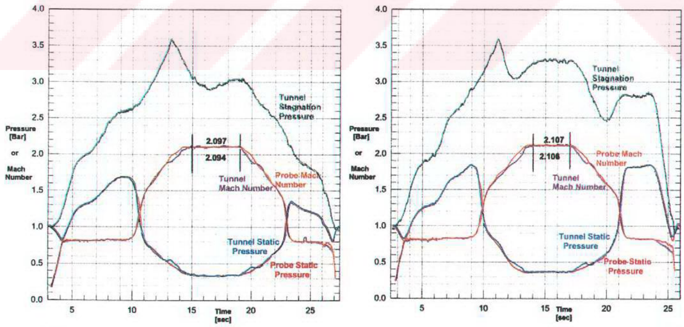

a) b)

Figure 4.21: Static pressure probe measurements with the insert and different streamwise location of measurement points at $P_m/P = 3$.

4.3.2.3. Probe traversing insert present, same measurement locations along the tunnel axis at $P_m/P = 2.3$:

In this case, similar to the previous study cases, the probe extension adaptor is mounted to the probe support in order to bring the probe static holes to the same location as the wall static pressure tap.

Figures 4.22.a and 4.22.b show results of two similar experiments performed the same day with the same test conditions for this configuration. According to results, this case shows perfect agreement in Mach numbers obtained from two static pressure sources.

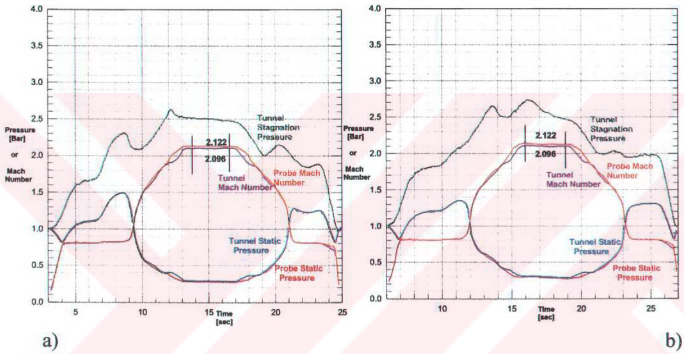

Figure 4.22: Static pressure probe measurements with the insert and the same streamwise location of measurement points at $P_m/P = 2.3$.

4.3.2.4. Probe traversing insert present, same measurement locations along the tunnel axis at $P_m/P = 3$:

The experiments, whose graphs are shown in Figures 4.23.a and 4.23.b, are done with the same conditions. In these two runs, there is a little discrepancy between the two measured static pressures and calculated Mach numbers. However, the level of the discrepancy in Mach numbers is much more smaller than that in the same configuration mentioned in section 4.3.1.2.

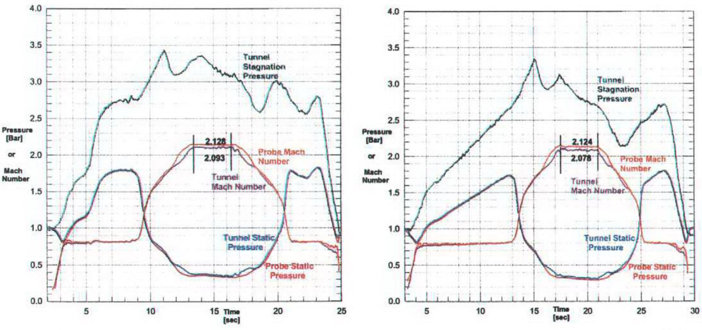

a) b)

Figure 4.23: Static pressure probe measurements with the insert and the same streamwise location of measurement points at $P_m/P = 3$.

4.3.2.5. Probe traversing insert absent, different measurement locations along the tunnel axis at $P_m/P = 2.3$:

In the third configuration, the probe traversing insert is removed from the test section. and the static pressure probe is mounted using the tunnel model support.

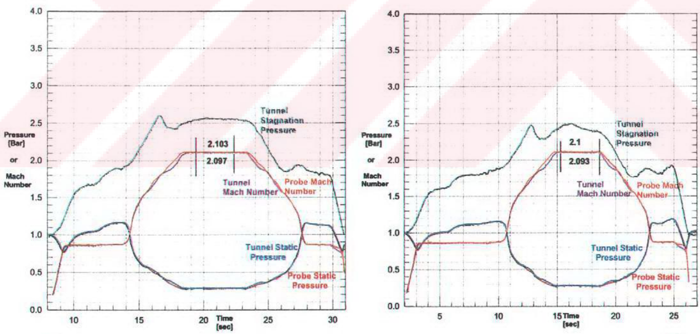

a) b)

Figure 4.24: Static pressure probe measurements without the insert and different streamwise location of measurement points at $P_m/P = 2.3$

The Figures 4.24.a and 4.24.b show the time histories of pressures and the Mach numbers with this configuration. As can be seen from the figure there is a good agreement between the two static pressures and hence the Mach numbers calculated. During the steady flow conditions the difference between the two Mach numbers in the test section is less than 0.01.

4.3.2.6. Probe traversing insert absent, different measurement locations along the tunnel axis at $P_m/P = 3$:

Experiments, shown in Figures 4.25.a and 4.25.b, are done on the same day and same conditions. As the previous case, there is a good agreement between the two static pressures and the Mach numbers calculated.

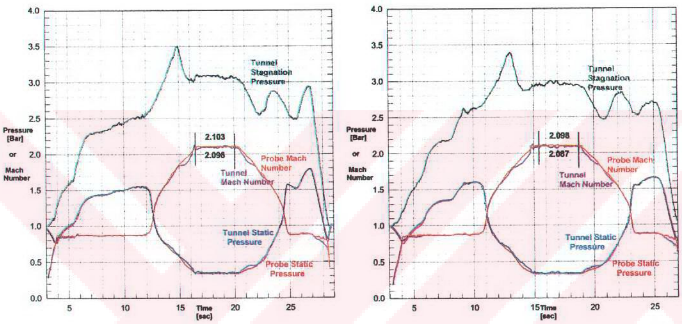

a) b)

Figure 4.25: Static pressure probe measurements without the insert and different streamwise location of measurement points at $P_m/P = 3$

4.3.2.7. Probe traversing insert absent, same measurement locations along the tunnel axis at $P_m/P = 2.3$:

In this last configuration, the probe is mounted on the model support with another adaptor to bring the location of its holes forward to match with that of the wall static pressure tap. The experiments, whose graphs are shown in Figure 4.26.a and 4.26.b, are done on the same day and same conditions. In these two runs there is a slight discrepancy between the two measured static pressures and thus the two Mach numbers calculated. The differences between the Mach numbers are 0.02 in both of the experiments.

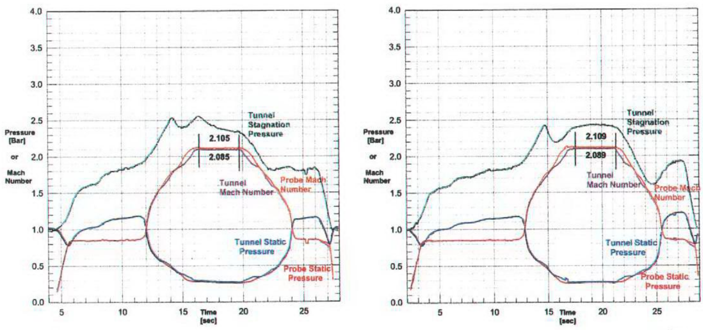

a) b)

Figure 4.26: Static pressure probe measurements without the insert and the same streamwise location of measurement points at $P_m/P = 2.3$

4.3.2.8. Probe traversing insert absent, same measurement locations along the tunnel axis at $P_m/P = 3$:

Experiments, shown in Figures 4.27.a and 4.27.b, are done on the same day and same conditions. According to the figures, there is a slightly larger difference between the Mach numbers than that in the previous case. During the steady flow conditions the difference between the two Mach numbers in the test section is about 0.03.

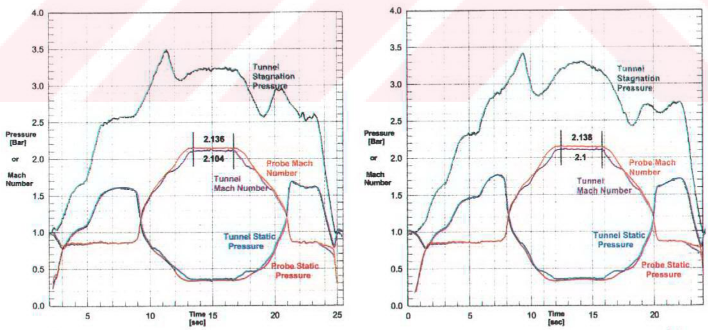

a) b)

Figure 4.27: Static pressure probe measurements without the insert and the same streamwise location of measurement points at $P_m/P = 3$.

Finally, it is concluded that the time histories of Mach numbers for all of the above cases show constant values and the leakage is eliminated by changing the bolt of the static pressure tap.

4.4 Repeatability of Results

Results are classified in different subgroups and shown in table 1. The average Mach number term in the table is calculated by using tunnel stagnation pressure and probe static pressure. According to the table, the total pressure ratio in the stagnation chamber does not affect the Mach number. Generally speaking, results are consistent in the configuration group in terms of the deviations.

Table 1. Different experimental conditions and results

Experiment condition	Number of experiment	Average Mach number	Mach RMS value	Average Mach – Mach RMS	Average Mach + Mach RMS
$P_m/P = 2.3$	12	2.108	0.01229	2.09571	2.12029
$P_m/P = 3.0$	11	2.109	0.01905	2.08995	2.12805
PPDL	6	2.122	0.00356	2.11844	2.12556
PPSL	6	2.095	0.00208	2.09292	2.09708
PADL	6	2.097	0.00611	2.09089	2.10311
PASL	5	2.121	0.01514	2.10586	2.13614
$P_m/P = 2.3$ & PPDL	2	2.091			
$P_m/P = 3.0$ & PPDL	4	2.097			
$P_m/P = 2.3$ & PPSL	4	2.120			
$P_m/P = 3.0$ & PPSL	2	2.126			
$P_m/P = 2.3$ & PADL	3	2.099			
$P_m/P = 3.0$ & PADL	3	2.095			
$P_m/P = 2.3$ & PASL	3	2.111			
$P_m/P = 3.0$ & PASL	2	2.137			

PPDL : Probe traversing insert present, different locations along the tunnel axis

PPSL : Probe traversing insert present, same locations along the tunnel axis

PADL: Probe traversing insert absent, different locations along the tunnel axis

PASL : Probe traversing insert absent, same locations along the tunnel axis

Since the number of experiments is limited, explanation of the statistical values should be considered carefully. Therefore, the root mean square (RMS) values of the subgroup are not calculated when acceptable number of experiment is less than 5. Unbiased standard deviation is used in the calculations when there are less then 20 experimental data. Especially in the PASL configuration the standard deviation is higher. According to these results and limited experimental data, it is not accurate to discuss a tendency of the results.

In the fifth and sixth columns of the table, the range of Mach number is calculated by adding and subtracting RMS values from average Mach numbers. The variation of the range of the Mach numbers according to four different probe-tap combinations is shown in figure 4.28.

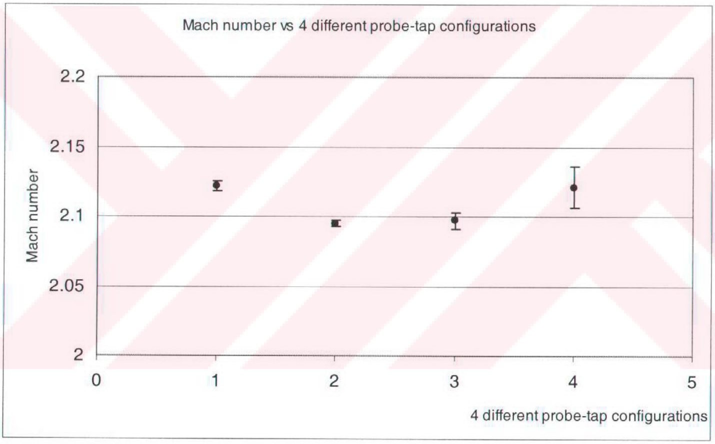

Figure 4.28: The variation of the range of the Mach numbers according to four different probe-tap combination

According to the table and Figure 4.28, the case, in which probe traversing insert is present and the probe and the tap are on the same measurement locations along the tunnel axis, therefore RMS value is minimum, is chosen as the optimum case and 20 additional experiments with the same conditions are done. In these experiments, P_m/P ratio is selected as 2.3. Although the previous RMS value is 0.00208 for this configuration, it is found to be 0.00648 according to the last set of data obtained from 20 experiments.

5. CONCLUSION

In this study, pressure measurements are performed to determine the flow quality within the test section of the 150x150 Trisonic Wind Tunnel using total or static pressure probes attached to a traversing system.

The results can be summarized as follows:

- The distribution of Mach number is quite uniform within the freestream region.
- The wall boundary layer thickness is about 3 cm on both the upper and the lower walls.
- The total pressure probe influences the wall static pressure when it is brought down closer to the wall for the near sonic case of Mach 1.05.
- There is good agreement between the measured values from the wall static tap and the probe in static pressure measurements.
- The Mach numbers obtained from the probe seems to be closer to the design value.
- The RMS value of the probe Mach number is acceptable for such a supersonic wind tunnel.

REFERENCES

[1] **Ferrari, C., Tricomi, F. G.,** 1968. Transonic Aerodynamics, Academic Press Inc., New York

[2] **Ramm, J. H.,** 1990. Fluid Dynamics for the Study of Transonic Flow, Oxford University Press, New York.

[3] **Moulden, T. H.,** 1984. Fundamentals of Transonic Flow, Robert E. Krieger Publishing Co., Inc., Florida.

[4] **Blackwell, Jr. J. A.,** 1981. Experimental testing at transonic speeds. *Proceedings of Transonic Perspective Symposium*, NASA/Ames Research Center California, Vol.81, pp 189-238.

[5] **Pope, A., Goin, K. L.,** 1965. High-Speed Wind Tunnel Testing, Robert E. Krieger Publishing Co., Inc., Florida.

[6] **Gulacti, B.,** 1988. İTÜ 150 x 150 mm Trisonik Rüzgar Tüneli Kalibrasyonu ve Bazı Deneyler, *Yüksek Lisans Tezi,* İ.T.Ü. Fen Bilimleri Enstitüsü, İstanbul.

[7] **Elbay, M. K.,** 2001. İTÜ 150 x 150 mm Trisonik Rüzgar Tünelinin Çalıştırma Kalibrasyonu, Yazılımı ve Bir Uygulama, *Doktora Tezi,* İ.T.Ü. Fen Bilimleri Enstitüsü, İstanbul.

[8] **Acar, M., Atli, V.,** 2002 Calibration Procedure of the Three-component Sting Type Balance for the Investigation of the Cone Flow at a Supersonic Mach Number. *Proceedings of 3rd International Symposium on Strain Gauge Balances*, Darmstadt-Germany.

[9] **Fenercioglu, I.,** 2001. An experimental investigation of aerodynamics characteristics of a high speed projectile with a forward-facing cavity, *Yüksek Lisans Tezi,* İ.T.Ü. Fen Bilimleri Enstitüsü, İstanbul.

[10] **Sayin, A., Yuceil, K. B., Cetiner – Yildirim, O.,** 2003. Determination of Transonic Flow Properties of A Trisonic Wind Tunnel For Its Use in Missile Aerodynamics., *Proceedings of 7th International Symposium on Fluid Control, Measurement and Visualization*, Sorrento-Italy.

RESUME

Ahmet Sayın was born in Bafra on January 27, 1979. He was graduated from Bafra Lisesi in 1995 and entered to the Aeronautical Engineering Department of the Middle East Technical University in 1996. In 2001 he received his Bachelor of Science Degree in Aeronautical Engineering and enrolled in the Master of Science program of the Institute of Science and Technology of ITU. Since November 2001, he is employed as a research assistant at the Trisonic Research Center.